



Impacts of organic aerosols and its oxidation level on CCN activity from measurement at a suburban site in China

Fang Zhang¹, Zhanqing Li^{1,2}, Yanan Li¹, Yele Sun³, Zhenzhu Wang⁴, Ping Li¹, Li Sun⁵, Pucai Wang⁶, Maureen Cribb², Chuanfeng Zhao¹, Tianyi Fan¹, Xin Yang¹, and Qingqing Wang³

¹State Key Laboratory of Earth Surface Processes and Resource Ecology, College of Global Change and Earth System Science, Beijing Normal University, 100875 Beijing, China

²Earth System Science Interdisciplinary Center and Department of Atmospheric and Oceanic Science, University of Maryland, College Park, Maryland, USA

³State Key Laboratory of Atmospheric Boundary Layer Physics and Atmospheric Chemistry, Institute of Atmospheric Physics, Chinese Academy of Sciences, 100029 Beijing, China

⁴Key Laboratory of Atmospheric Composition and Optical Radiation, Anhui Institute of Optics and Fine Mechanics, Chinese Academy of Sciences, 230031 Hefei, China

⁵Liaoning Weather Modification Office, 112000 Shenyang, China

⁶Key Laboratory of Middle Atmosphere and Global Environment Observation (LAGEO), Institute of Atmospheric Physics, Chinese Academy of Sciences, 100029 Beijing, China

Correspondence to: Zhanqing Li (zli@atmos.umd.edu)

Received: 14 May 2015 – Published in Atmos. Chem. Phys. Discuss.: 15 June 2015

Revised: 5 February 2016 – Accepted: 13 March 2016 – Published: 2 May 2016

Abstract. This study is concerned with the impacts of organic aerosols on cloud condensation nuclei (CCN) activity based on field measurements made at a suburban site in Northern China. The sensitivity of the estimated CCN number concentration (N_{CCN}) to both volume fraction of organic material (x_{org}) and aerosol oxidation level (using f_{44} , the fraction of m/z 44 in aerosol organic material) are examined. A strong dependence of CCN number concentration (N_{CCN}) on the x_{org} and f_{44} was noted. The sensitivity of N_{CCN} to volume fraction of organics increased with increasing x_{org} . The impacts of the aerosol particles oxidation or aging level on estimating N_{CCN} were also very significant. When the particles were mostly composed of organics ($x_{org} > 60\%$), the N_{CCN} at the supersaturation of 0.075 and 0.13% was underestimated by 46 and 44%, respectively, if aerosol particles were freshly emitted with primary organics ($f_{44} < 11\%$); the underestimation decreased to 32 and 23% at the corresponding supersaturations, however, if the particles were with more hygroscopic secondary organics ($f_{44} > 15\%$). The N_{CCN} at the supersaturation of 0.76% was underestimated by 11 and 4%, respectively, at $f_{44} < 11$ and $f_{44} > 15\%$. However, for the particles composed of low organics (e.g., $x_{org} < 40\%$), the

effect caused by the f_{44} was quite insignificant both at high and low supersaturations. This is because the overall hygroscopicity of the particles is dominated by inorganics such as sulfate and nitrate, which are more hygroscopic than organic compounds. Our results indicated that it would decrease the uncertainties in estimating N_{CCN} and lead to a more accurate estimation of N_{CCN} to increase the proportion of secondary organics, especially when the composition of the aerosols is dominated by organics. The applicability of the CCN activation spectrum obtained at Xinzhou to the Xianghe site, about 400 km to the northeast of Xinzhou, was investigated, with the aim of further examining the sensitivity of N_{CCN} to aerosol type. Overall, the mean CCN efficiency spectrum derived from Xinzhou performs well at Xianghe when the supersaturation levels are $> 0.2\%$ (overestimation of 2–4%). However, N_{CCN} was overestimated by $\sim 20\%$ at supersaturation levels of $< 0.1\%$. This suggests that the overestimation is mainly due to the smaller proportion of aged and oxidized organic aerosols present at Xianghe compared to Xinzhou.

1 Introduction

To reduce the uncertainty of aerosol indirect effects on the radiative balance of the atmosphere, it is important to gain a good knowledge of the ability of aerosol particles to form cloud condensation nuclei (CCN) at the typical supersaturations found in the atmosphere. The CCN activity of aerosol particles is governed by the Köhler theory (Köhler, 1936). This theory determines CCN from aerosol particle size and physicochemical properties, which include the molar volume, activity coefficient, and effect on surface tension (McFiggans et al., 2006). These properties, however, are difficult to measure.

Researchers have proposed single-parameter models to parameterize the CCN activation and hygroscopicity of multi-component aerosols (Hudson and Da, 1996; Rissler et al., 2006; Petters and Kreidenweis, 2007; Wex et al., 2007). Field experiments have been conducted with the aim of better characterizing particle physicochemical parameters influencing cloud CCN activation. Due to the large spatial variability of aerosol types and compositions, the CCN activation efficiency varies greatly over different regions. CCN number concentrations (N_{CCN}) can often be better predicted in the background atmosphere (Chuang et al., 2000; Dusek et al., 2003; VanReken et al., 2003; Snider et al., 2003; Rissler et al., 2004; Gasparini et al., 2006; Stroud et al., 2007; Bougiatioti et al., 2009).

The largest errors are associated with urban emissions (Sotiropoulou et al., 2007). This is likely due to the organics component of aerosol particles, which have the largest uncertainty and are not fully understood. Biomass burning aerosols and secondary organics formed from the oxidation of common biogenic emissions are often more difficult to activate (Mircea et al., 2005; VanReken et al., 2005; Lee et al., 2006; Varutbangkul et al., 2006; Clarke et al., 2007; Rose et al., 2010; Engelhart et al., 2012; Paramonov et al., 2013; Latham et al., 2013; Mei et al., 2013b; Zhang et al., 2014). Particles with aged/oxidized secondary organic components (e.g., organic acids) have been shown to be more hygroscopic (Raymond and Pandis, 2002; Hartz et al., 2006; Bougiatioti et al., 2011) but still much less hygroscopic than inorganic species. The sensitivity of estimated N_{CCN} to organics has been examined in a number of recent studies (Wang et al., 2008; Reutter et al., 2009; Ervens et al., 2010; Kammermann et al., 2010; Ward et al., 2010; Zhang et al., 2012; Mei et al., 2013a). It is widely known that the estimated N_{CCN} is sensitive to changes in organics due to the latter's complex components. The amounts and hygroscopicity parameter of organics (κ_{org}) vary substantially and lead to significant biases in estimating CCN concentrations and aerosol indirect forcing (Sotiropoulou et al., 2007; Hings et al., 2008; Liu and Wang, 2010). Therefore, field investigations regarding CCN activity and organics impacts, especially in heavily polluted regions, are pivotal to better parameterize CCN in climate models.

Northern China is a fast developing and densely populated region of China, where aerosol loading is high (Li et al., 2007, 2011), the particle composition is complex, and severe haze pollution episodes are common (Guo et al., 2014). In recent years, CCN measurements have been collected during field campaigns carried out in the region (Wiedensohler et al., 2009; Gunthe et al., 2011; Yue et al., 2011; Deng et al., 2011, 2013; Zhang et al., 2014). These studies have presented different perspectives on the influence of particle size and composition on CCN activity. For example, Deng et al. (2013) evaluated various schemes for CCN parameterization and recommended that the particle number size distribution (PSD) together with inferred mean size-resolved activation ratios can be used to estimate CCN number concentrations without considering the impact of particle composition. However, Zhang et al. (2014) demonstrated that the 30–40 % uncertainties in N_{CCN} are mainly associated with changes in particle composition. None of the above-mentioned studies have investigated the impact of organics on estimating N_{CCN} in Northern China. Zhang et al. (2012) noted a more significant influence of organics on CCN activity but without concerning the influences of particles oxidation or aging on CCN activity; in addition, the campaign average mass fraction of organics in their study was < 20 %.

The aim of this paper is to examine the sensitivity of CCN activity to aerosol physicochemical properties (especially aerosols containing large amounts of organics, as well as the oxidation level) and also to see how much uncertainty is incurred by applying the CCN efficiency spectra measured at one site to another site in a heavily polluted region. The instrumentation and data used in the study are described in Sect. 2. The method for calculating the hygroscopicity parameter (κ_{chem}) is introduced in Sect. 3. The applicability of the CCN activation spectrum obtained at Xinzhou to the Xianghe site was also investigated in this section, with the aim of further examining the sensitivity of N_{CCN} to aerosol type. Conclusions from the study are given in Sect. 5.

2 Measurements and data

An intensive observation period field campaign similar to the Aerosol–CCN–Cloud Closure Experiment (AC^3Exp) (Zhang et al., 2014), called the Atmosphere, Aerosol, Cloud, and CCN (A^2C^2) experiment, was conducted from 22 July to 26 August of 2014 at Xinzhou (38.24° N, 112.43° E; 1500 m above sea level), a city with a population of 0.51 million in Northern China. The site is located about 360 km southwest of the metropolitan Beijing area and about 10 km south of the local town center. The site is surrounded by agricultural land (e.g., corn) with little local pollution plums from motor vehicles and industrial activities. Sitting between two mountains (Taihang Mountain to the east and Lüliang Mountain to the west), the site also experiences air masses from Xinzhou to the north and from Taiyuan to the south, the cap-

ital of Shanxi Province. Air masses from the northeast and southwest dominate over the site during summer. Depending on the wind direction, measurements at the Xinzhou site can detect air parcels of urban, rural, or mixed origins, including both fresh biogenic emissions around the site and aged aerosols from advection.

2.1 Instruments and measurements

During the field campaign, a scanning mobility particle sizer (SMPS), combined with a Droplet Measurement Technologies cloud condensation nuclei counter (DMT-CCN_C; Lance et al., 2006), was used for size-resolved CCN measurements as well as PSD measurements. The measured aerosol PSD is within the size range of 14–600 nm. Aerosol chemical composition was measured simultaneously by an Aerodyne aerosol chemical speciation monitor (ACSM; Sun et al., 2012).

The aerosol inlet for the size distribution measurements was equipped with a TSI Environmental Sampling System (model 3031200), which consists of a sharp-cut PM₁ cyclone and a bundled nafion dryer. The size-resolved CCN efficiency spectra were measured by coupling the DMT-CCN_C used with the SMPS (Rose et al., 2008). In this step, the particles are rapidly dried with RH < 30% upon entering the differential mobility analyzer (DMA). Thus, size selection is effectively performed under dry conditions. The nafion dryer and the sheath air inside the DMA are sufficient to remove residual water associated with the ambient particles. Relative deviations in particle diameter should be < 1%. The sample flow exiting the DMA was split into two parts: 0.3 lpm for the CPC and 0.5 lpm for the CCN counter (CCN_C). The DMA, controlled by TSI-AIM software, scanned one size distribution every 5 min. The CCN_C was operated at a total flow rate of 0.5 lpm with a sheath-to-aerosol flow ratio of 10. The inlet RH for CCN_C was < 30%. During the field campaign, the mean sample temperature and pressure measured by CCN_C sensors was (24.3 ± 1.4) °C and (898.4 ± 11.7) hPa. The supersaturations levels of CCN_C were calibrated with ammonium sulfate before and after the field campaign, following the procedures outlined in Rose et al. (2008). During each CCN measurement cycle, calibrated effective supersaturations were set at 0.075, 0.13, 0.17, 0.39, and 0.75%. The overall relative error (1σ) for the supersaturation levels was estimated to be < 3.5%. The completion of a full measurement cycle took 50 min (10 min for each supersaturation level).

The measurement of non-refractory submicron aerosol species including organics, sulfate, nitrate, ammonium, and chloride were made with an ACSM. During the field campaign, ambient aerosols were drawn inside through a 1/2 inch (outer diameter, the inner diameter is 0.38 inch) stainless steel tube at a flow rate of ~ 3 L min⁻¹, of which ~ 84 cc min⁻¹ was sub-sampled into the ACSM. An URG cyclone (model URG-2000-30ED) was also positioned in

front of the sampling inlet to remove coarse particles with a cut-off size of 2.5 μm. Before sampling into the ACSM, aerosol particles were dried using a silica gel desiccant. The residence time in the sampling tube was ~ 5 s. The ACSM was operated at a time resolution of ~ 15 min with a scan rate of mass spectrometer at 500 ms amu⁻¹ from *m/z* 10 to 150. Regarding the calibration of the ACSM, mono-dispersed, size-selected 300 nm ammonium nitrate particles within a range of concentrations were sampled into both the ACSM and a condensation particle counter (CPC). The ionization efficiency (IE) was then determined by comparing the response factors of the ACSM to the mass calculated with known particle size and number concentrations from the CPC. More detailed descriptions of the operation and calibration of the ACSM are given in Sun et al. (2012) and Ng et al. (2011). The campaign averaged mass concentration of PM₁ is 31.6 μg m⁻³.

In addition to the ACSM, the black carbon (BC) in PM_{2.5} was simultaneously measured at a time resolution of 5 min by a seven-wavelength aethalometer (model AE31, Magee Scientific Corporation). The campaign averaged mass concentration of BC is ~ 2.5 μg m⁻³. During the experiment, the campaign area was generally hot and dry, with an average temperature of 21.6 °C and an average ambient RH of 69.5%.

2.2 Data

The raw CCN data were first filtered according to instrument recorded parameters (e.g., temperature and flow). For example, if the relative difference between the actual and preset sample flows was larger than 4%, the data were flagged as invalid. The data were also excluded if the “temperature stability” was flagged as “0”. Here, the “temperature stability” refers to the *T*₁, *T*₂, and *T*₃ in the cloud chamber of the CCN_C, which is set to obtain the target supersaturations. If the average differences between preset *T*₁, *T*₂, and *T*₃ and the measured values are larger than 0.4 C, the “temperature stability” is flagged as “0”. Thus, the data are invalid and will be removed. A multiple charge correction and transfer function (Deng et al., 2011) is applied to each PSD as well as to the CCN efficiency spectrum. Size-resolved CCN and PSD data, measured with a DMT-CCN_C and a SMPS (with a particle size range of 10–700 nm) on 7–21 July 2013 at Xianghe (Zhang et al., 2014), are used in this study for comparisons with CCN activity at the Xinzhou site. Aerosol mass concentrations were processed using the ACSM standard data analysis software (version 1.5.3.0). Detailed procedures for the data analysis have been described by Ng et al. (2011) and Sun et al. (2012). The size-resolved CCN activation ratio (size-resolved AR) is defined as the $dN_{CCN} / d\log D_p$ divided by the $dN_{CN} / d\log D_p$. These values were measured by SMPS/DMT-CCN_C with particle size selection in the DMA. The bulk activation ratio (bulk AR) is defined as the total CCN concentration divided by the total CN concentration.

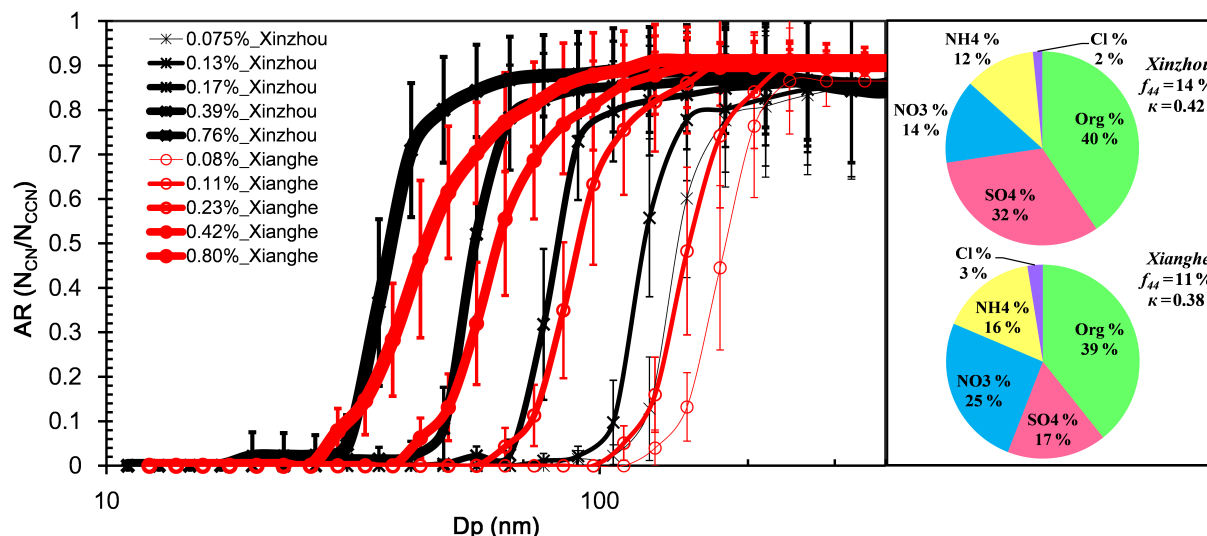


Figure 1. Mean CCN efficiency spectra at the Xinzhou site (black lines with asterisks) measured from 22 July to 26 August 2014 and at the Xianghe site (red lines with circles) site measured from 7 to 21 July 2013 for different supersaturation levels. Error bars representing 1 standard deviation are shown. Right panels show particle chemical composition in terms of mass concentration fractions at Xinzhou (top panel) and Xianghe (bottom panel) during their respective observation periods. The campaign average mass concentration of PM₁ is 31.6 and 72.4 $\mu\text{g m}^{-3}$ at Xinzhou and Xianghe, respectively. Note that the preset supersaturation levels were 0.07, 0.1, 0.2, 0.4, and 0.8 % at both sites, but effective supersaturation levels showed slightly different after calibration.

The total CCN and CN number concentrations are integrated by the measured CCN and CN size distribution, respectively, over the whole size range.

3 Derivation of κ_{chem}

In this study, we calculate κ_{chem} based on bulk chemical composition observations made during the field campaign. The method is very similar to that used by Zhang et al. (2014). As proposed by Petters and Kreidenweis (2007), κ_{chem} can be predicted using a simple mixing rule based on chemical volume fractions for a given internal mixture:

$$\kappa_{\text{chem}} = \sum_i \varepsilon_i \kappa_i, \quad (1)$$

where κ_i and ε_i are the hygroscopicity parameter and volume fraction, respectively, for the individual (dry) components in the mixture and i is the number of components in the mixture.

Measurements from the ACSM in Xinzhou show that the composition of submicron particles was dominated by organics, followed by sulfate, ammonium, and nitrate. The contribution of chloride was negligible (volume fraction of about <2%). The analysis of the anion and cation balance suggests that anionic species (NO_3^- , SO_4^{2-}) were essentially neutralized by NH_4^+ over the relevant size range. For refractory species, BC represented a negligible fraction of the total submicron aerosol volume (<3%). Sea salt and dust are usually coarse mode particles with particle sizes >1 μm (Whitby,

1978). The contribution of such types of aerosols is thus expected to be negligible for sizes <1 μm . Therefore, the submicron particles measured by the ACSM mainly consisted of organics, $(\text{NH}_4)_2\text{SO}_4$, and NH_4NO_3 . The particle hygroscopicity is thus the volume average of the three participating species:

$$\kappa_{\text{chem}} = \kappa_{\text{org}} \varepsilon_{\text{org}} + \kappa_{(\text{NH}_4)_2\text{SO}_4} \varepsilon_{(\text{NH}_4)_2\text{SO}_4} + \kappa_{\text{NH}_4\text{NO}_3} \varepsilon_{\text{NH}_4\text{NO}_3}. \quad (2)$$

Here, the values of κ for $(\text{NH}_4)_2\text{SO}_4$ and NH_4NO_3 are 0.61 and 0.67, respectively. The following linear function derived by Mei et al. (2013a) was used to estimate κ_{org} in this study: $\kappa_{\text{org}} = 2.10 \times f_{44} - 0.11$, where f_{44} is the fraction of m/z 44 in total organics. The mean value of κ_{org} during the field campaign is 0.115 ± 0.019 .

4 Results and discussion

4.1 CCN efficiency spectra

During the field campaign at the Xinzhou site, ~ 790 size-resolved CCN efficiency spectra at five supersaturation levels ranging from 0.075 to 0.76 % were measured. Figure 1 shows campaign averaged spectra of the measured CCN efficiency at Xinzhou for supersaturation levels of 0.075, 0.13, 0.17, 0.39, and 0.76 %. The observed averaged CCN efficiency spectra during Xianghe campaign in summer 2013 are also shown. Note that the maximum activation fraction (MAF) for Xianghe site showed in Fig. 1 is slight lower than that

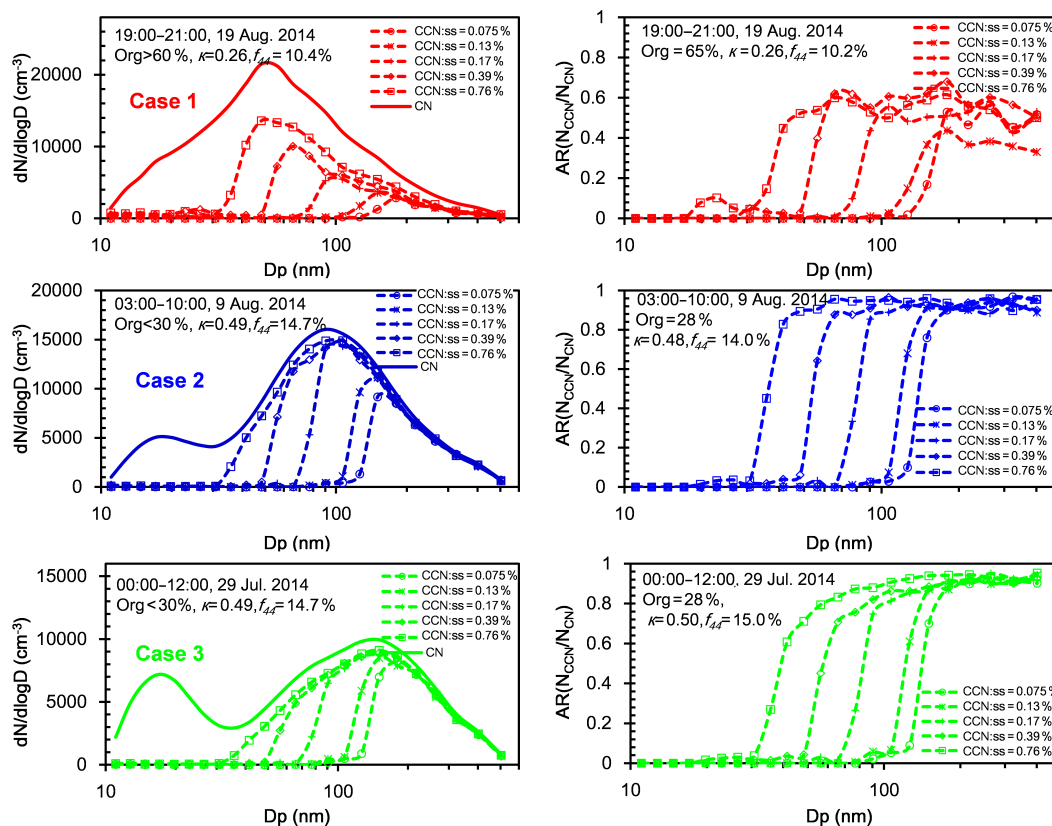


Figure 2. Particle number size distribution (PSD) and CCN size distributions (left panels) and CCN efficiency spectra (right panels) at different supersaturation levels for Case 1 (upper panels; 19 August 2014, 19:00–21:00 LT), Case 2 (middle panels; 9 August 2014, 03:00–10:00 LT), and Case 3 (bottom panels; 29 July 2014, 00:00–12:00 LT). Total CN number concentrations are 16 671, 12 869, and 10 134 cm⁻³ for Case 1, Case 2, and Case 3, respectively. Mass concentrations of PM₁ are 28.36, 81.45, and 78.73 $\mu\text{g m}^{-3}$ for Case 1, Case 2, and Case 3, respectively.

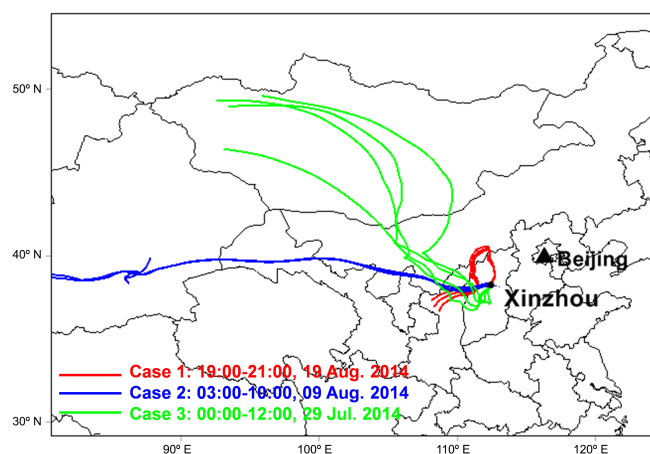


Figure 3. Five-day back trajectories for Case 1 (in red), Case 2 (in blue), and Case 3 (in green) calculated using the Hybrid Single-Particle Lagrangian Integrated Trajectory model with National Centers for Environmental Prediction reanalysis data. The arrival height of the trajectories at the Xinzhou site was at the surface.

we plotted in Zhang et al. (2014). Because some data points with MAF value > 1 were also included previously, larger mean MAF resulted. However, in this paper the data points with MAF > 1.0 were forced to 1 when $D_p > 300$ nm, which could be completely activated at even lower supersaturations, but the MAF would never be larger than 1.0. In Fig. 1, the right panels show the mass concentration fraction of particle chemical compositions at Xinzhou (top panel) and Xianghe (bottom panel) during their respective observation periods. Significant differences in size-resolved CCN efficiency spectra at the two sites are seen. Aerosol particles at Xinzhou activate more efficiently (higher values of AR) at a given particle diameter (D_p) for the same supersaturation level. In other words, a larger D_p was required to reach the same activation efficiency at Xianghe. This suggests that aerosol properties at each site differ.

The slope of AR with respect to diameters near D_p when $AR = 50\%$ (defined here as the cut-off diameter, D_{cut}) provides information about the heterogeneity of the composition for size-resolved particles. For an ideal case when all CCN-active particles have the same composition and size, a

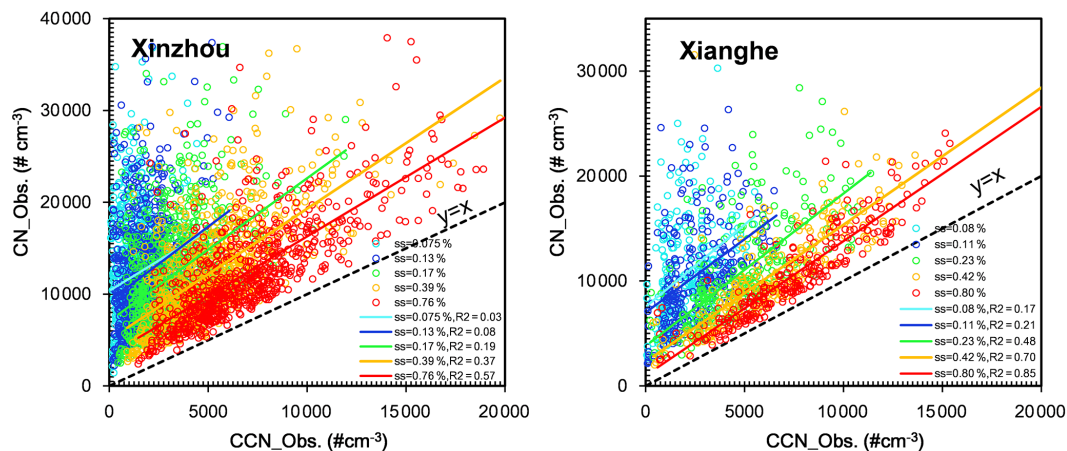


Figure 4. Measured N_{CN} as a function of measured N_{CCN} for different supersaturation levels at the Xinzhou (left panel) and Xianghe (right panel) sites. The scatter plot between CCN_{Obs} and CN_{Obs} were fitted with a linear function (in colored lines) and R^2 refer to the correlations of them.

steep change in AR from 0 to 1 would be observed as D_p reached D_{cut} . A gradual increase in size-resolved AR with D_p suggests that aerosol particles have different hygroscopicities. The steeper slopes of AR around D_{cut} observed at Xinzhou suggest that the particle composition was less heterogeneous with more hygroscopicity than particles at the Xianghe site. This can be partially explained by the magnitudes of the mean κ_{chem} at the two sites (0.42 at Xinzhou and 0.38 at Xianghe). Also, the f_{44} is greater at Xinzhou than at Xianghe. The m/z 44 signal is mostly due to acids (Takegawa et al., 2007; Duplissy et al., 2011) or acid-derived species, such as esters. f_{44} is closely related to the organic oxidation level (Aiken et al., 2008). Oxidized/aged acids are generally more hygroscopic and easily activated. Moreover, the primary inorganic particles at the Xinzhou site are sulfates, with a mass fraction that is twice greater than that measured at Xianghe. Therefore, particles at the Xinzhou site consist of more hygroscopic sulfate-dominant inorganics and aged/oxidized secondary organics and can thus be more efficiently activated at a given D_p , as shown in Fig. 1.

4.2 Air mass influences on CCN activity: a case study

Because air mass back trajectories combined with ambient air measurements can be used for analyzing large-scale air pollutant transport and source identification at a receptor site (Stohl, 1996; Rousseau et al., 2004), in this study we calculated 5-day (120 h) back trajectories using the Hybrid Single-Particle Lagrangian Integrated Trajectory (HYSPPLIT) model (Draxler and Hess, 1998) with National Centers for Environmental Prediction (NCEP) reanalysis data. TrajStat software (Wang et al., 2009) has been used to calculate trajectories. The arrival height of the trajectories at the Xinzhou site was at the surface.

Three cases were selected to study air mass influences on CCN activity: (1) Case 1, 19 August 2014, 19:00–21:00 local

time (LT); (2) Case 2, 9 August 2014, 03:00–10:00 LT; and (3) Case 3, 29 July 2014, 00:00–12:00 LT. Each case is associated with a different CCN efficiency spectrum, i.e., top, middle, and bottom panels of Fig. 2 are for Cases 1, 2, and 3, respectively. Their respective back trajectories are shown in Fig. 3.

In Case 1, air trajectories (red line in Fig. 3) originated from the southwest and passed through northern Shaanxi Province and northwestern Shanxi Province, then rounded back to the site from the north/northeast. So, aerosols in this case are closely associated with air parcels north/northeast of the site. The trajectories were very short, suggesting that the air flow was slow during the observational period. Under these circumstances, aerosol loading would be largely impacted by local sources around the site. A high mass fraction of organics (> 60 %) with low f_{44} (~ 10 %) and κ_{chem} (< 0.3) values was measured during the observational period. Furthermore, the PSD showed one peak mode with $D_p = 56$ nm and a high N_{CN} ($\sim 1.7 \times 10^4 \text{ cm}^{-3}$), but low mass concentration of PM_{10} ($28.36 \mu\text{g m}^{-3}$). This suggests that particles may be composed of freshly emitted primary aerosols (the biogenic emissions from the plants and trees around the site). This type of aerosol is usually less hygroscopic with a single peak mode primarily composed of fine particles (Whitby, 1978; Hussein et al., 2005). These aerosols cannot activate efficiently. The MAF shown in the top right panel of Fig. 2 is less than 0.6 at all supersaturation levels for particles with $D_p > 300$ nm, indicating that the particles should be largely externally mixed aerosols.

In Case 2 (blue line in Fig. 3), air parcels moved rapidly from the west to the site. The site should then be influenced by the large-scale transport of air masses. For this case, aerosols contain a small amount of organics (< 30 %) but have high f_{44} (~ 14 %) and κ_{chem} values (~ 0.5). The PSD showed a double peak mode with an N_{CN} of

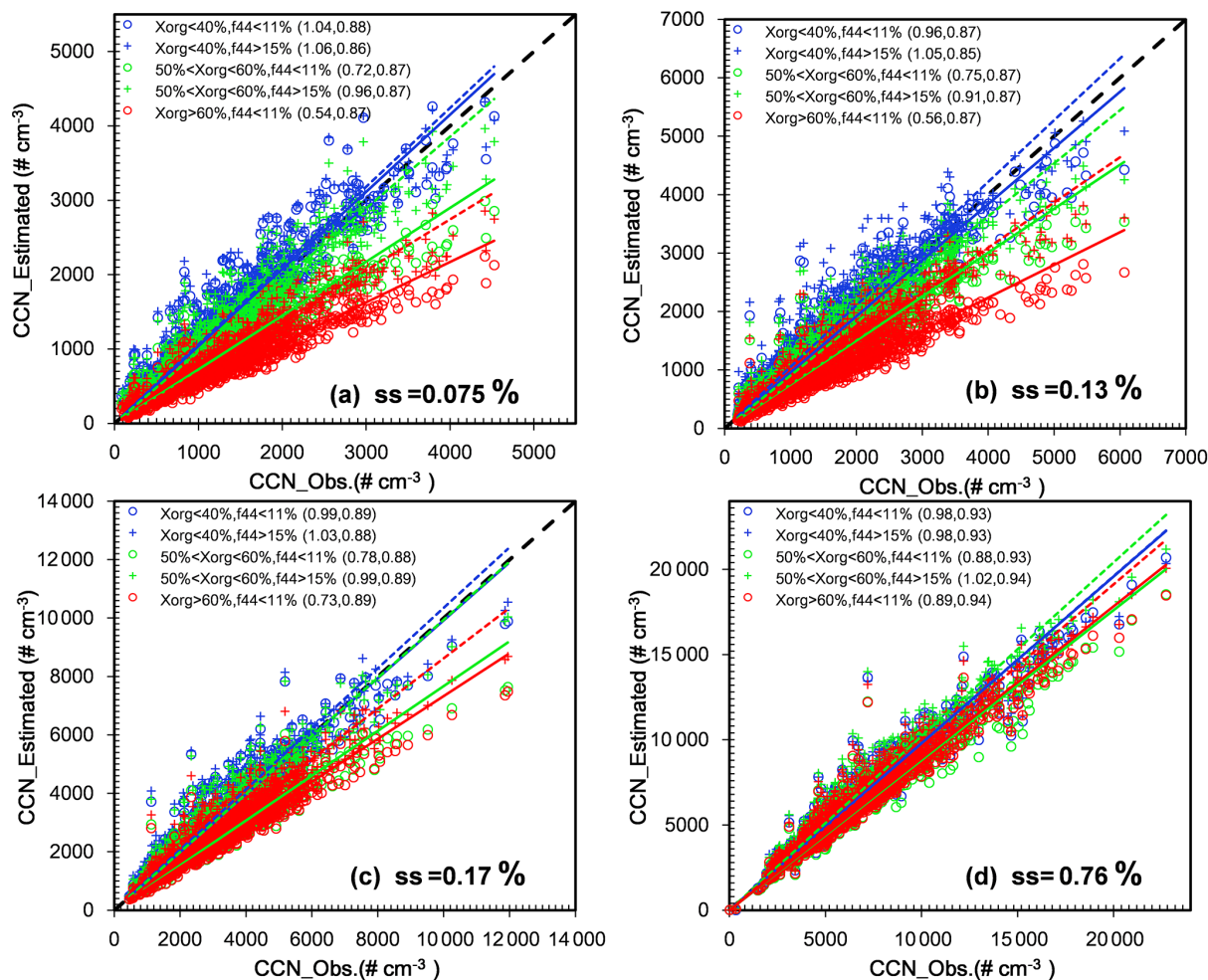


Figure 5. The sensitivity of N_{CCN} to both organics volume fraction (x_{org}) and oxidation level (using f_{44} , the fraction of m/z 44 in aerosol organic material) of organics at supersaturation levels of (a) 0.075, (b) 0.13, (c) 0.17, and (d) 0.76 % for cases when $x_{org} = 35\%$ (blue circles), 52 % (green circles), and 66 % (red circles). The size-resolved CCN data were sorted when the $x_{org} > 60\%$, $50\% < x_{org} < 60\%$, and $x_{org} < 40\%$, respectively, to do the sensitivity examination. Linear best-fit lines through each group of points are shown. Slopes and R^2 values are given in parentheses.

$\sim 1.3 \times 10^4 \text{ cm}^{-3}$ and a relatively high mass concentration of PM_{10} ($81.45 \mu\text{g m}^{-3}$). The double peak mode suggests that aerosols in this case are a mixture of aerosols from local sources and from other regions (Whitby, 1978; Dal Maso et al., 2007). Because aerosols are aged and oxidized during long-distance transport, these particles are usually composed of secondary organic and inorganic components with more hygroscopicity (Weber et al., 1999; Verver et al., 2000). These aerosols can activate efficiently. The MAF is close to 1 and the slopes of AR around D_{cut} are steep at all supersaturation levels (middle right panel of Fig. 2). This CCN efficiency spectrum is similar to the ideal spectrum of pure ammonium sulfate.

In Case 3 (green line in Fig. 3), air parcels traveled from the northwest to the site. Air masses arriving at the site in this case had passed over densely populated regions with more

heavy pollution. A gradual increase in size-resolved AR with D_p is seen (bottom right panel of Fig. 2). This is attributed to the diversity in aerosol hygroscopicity because of the complex nature of the chemical composition of aerosol particles.

4.3 Correlation of N_{CN} and N_{CCN}

Figure 4 shows N_{CN} as a function of N_{CCN} for different supersaturation levels at the Xinzhou and Xianghe sites. They showed high or moderate correlations at high supersaturation levels (e.g., $R^2 = 0.57$ at Xinzhou and $R^2 = 0.85$ at Xianghe at a supersaturation level of $\sim 0.8\%$) but quite poor correlations at low supersaturation levels. Although Andreae (2009) proposed using the relationship of CCN and CN, or even aerosol optical depth, to parameterize CCN in models, it would lead to large uncertainties especially when the supersaturations are low. It was noticed that there was an apparent

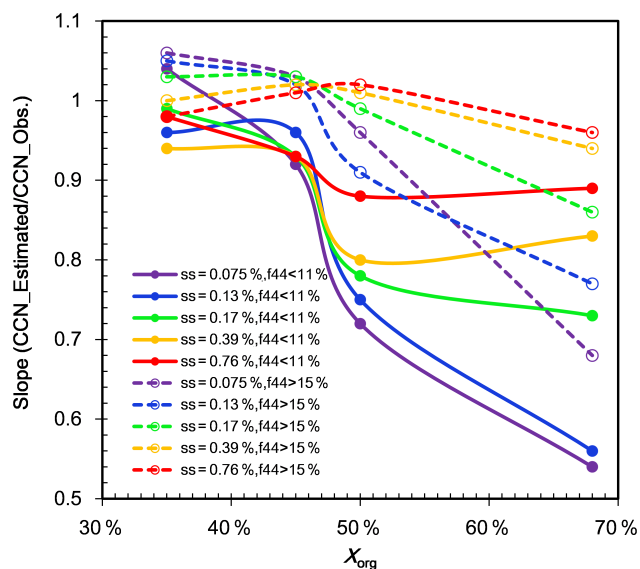


Figure 6. Slopes of the linear fit of estimated and observed N_{CCN} dependence on volume fraction of organics (x_{org}) at $f_{44} < 11$ and $f_{44} > 15$ % for different supersaturation levels. Mean values of the hygroscopic parameter κ_{chem} at $f_{44} < 11$ % when $x_{org} > 60$ %, $50 \% < x_{org} < 60$ %, $40 \% < x_{org} < 50$ %, and $x_{org} < 40$ % are 0.27, 0.34, 0.40, and 0.46, respectively, while at $f_{44} > 15$ % the value increased to 0.36, 0.42, 0.46, and 0.50, respectively.

higher degree of correlation at Xianghe site for each supersaturation than that derived at Xinzhou site. In light of the similar regimes from which the data are taken and the same instruments by which they have been collected, the discrepancy between Xianghe and Xinzhou should be caused largely by the spatial variations of aerosols types. These variations are primarily attributed to variations in aerosol particle size, i.e., the shape of the PSD as well as particle composition. As presented by Zhang et al. (2014), the relationship between bulk activation ratios and N_{CN} was complex under polluted conditions and was heavily dependent on the physicochemical properties of atmospheric aerosols.

4.4 Impact of x_{org} on N_{CCN}

Precise quantification of N_{CCN} is crucial for understanding aerosol indirect effects and characterizing these effects in models. A CCN closure study is useful to examine the controlling physical and chemical factors and to help verify experimental results. N_{CCN} is usually derived from measured aerosol properties, such as PSD and composition or hygroscopicity based on the Köhler theory. Achieving such closure under heavily polluted conditions is more challenging, especially due to the complex effects of organics on CCN activity. In this section, we examine the sensitivity of N_{CCN} to both volume fraction of organics (x_{org}) and oxidation or aging of organics based on measurement at Xinzhou site. During the observed period, aerosols at the Xinzhou site were

dominated by organics, with 12, 23, 39, and 25 % of the data points corresponding to $x_{org} > 60$ %, $50 \% < x_{org} < 60$ %, $40 \% < x_{org} < 50$ %, and $x_{org} < 40$ %, respectively. For the purpose of examining the sensitivity of estimated N_{CCN} to x_{org} and oxidation/aging level, we sorted the size-resolved CCN data when $x_{org} > 60$ %, $50 \% < x_{org} < 60$ %, $40 \% < x_{org} < 50$ %, and $x_{org} < 40$ %. Furthermore, for each level of x_{org} we tested the impacts on N_{CCN} estimation both from the most-oxidized (with f_{44} of higher than 15 %) and least-oxidized (those primary organic aerosols with f_{44} of lower than 11 %) organic particles. For example, the size-resolved CCN data points during the period when $x_{org} > 60$ and also $f_{44} > 15$ % were averaged to generate the averaged CCN efficiency spectra at the five supersaturations. Then we used the produced averaged CCN efficiency spectra to estimate N_{CCN} .

Estimated CCN size distributions at the five supersaturations were firstly calculated by multiplying the averaged CCN efficiency spectrum (by using the averaged CCN efficiency spectra, the aerosol particles were assumed with uniform chemical composition without considering the effects of the temporal variations of the activation curves on CCN activity) with the actually measured PSD. Then, we integrated the estimated CCN size distribution over the whole size range to generate estimated N_{CCN} . The measured CCN size distributions are integrated to produce the observed N_{CCN} .

Observed and estimated N_{CCN} at four supersaturation levels (0.075, 0.13, 0.17, and 0.76 %) were showed in Fig. 5. The data points presented more disperse and weaker correlations at lower supersaturations. The sensitivity of N_{CCN} to volume fraction of organics increased with increasing x_{org} . This is especially true for the case of these primary organic particles with $f_{44} < 11$ %: the slopes obtained from a linear fit of estimated and measured N_{CCN} in Fig. 6 decreased rapidly (almost with a decrease of ~ 50 %) when the x_{org} varied from < 40 to > 60 % at supersaturations of 0.075 %, while it did not exhibit a lot of reduction (merely ~ 10 %) along with the increasing of x_{org} at the supersaturation of 0.76 %. N_{CCN} was estimated most accurately at higher supersaturation levels. This is likely because a large fraction of particles was already CCN-active. Also, particle composition has relatively less influence on CCN activation at high supersaturations (Twohy and Anderson, 2008). For the oxidized or aged particles with $f_{44} > 15$ %, the slopes still follow the similar tendency with the variations of x_{org} at low and high supersaturations but changed more smoothly to the x_{org} attributing to the oxidized/aged organic particles being more hygroscopic.

However, the impacts of the aerosol particles oxidation level on estimating N_{CCN} were also very significant. For example, when the particles were composed by large amounts of organics ($x_{org} > 60$ %), the N_{CCN} at the supersaturation of 0.075 and 0.13 % was underestimated by 46 and 44 %, respectively, at $f_{44} < 11$ %, while the underestimation decreased to 32 and 23 % at the corresponding supersaturation level when $f_{44} > 15$ %. The N_{CCN} at $ss = 0.76$

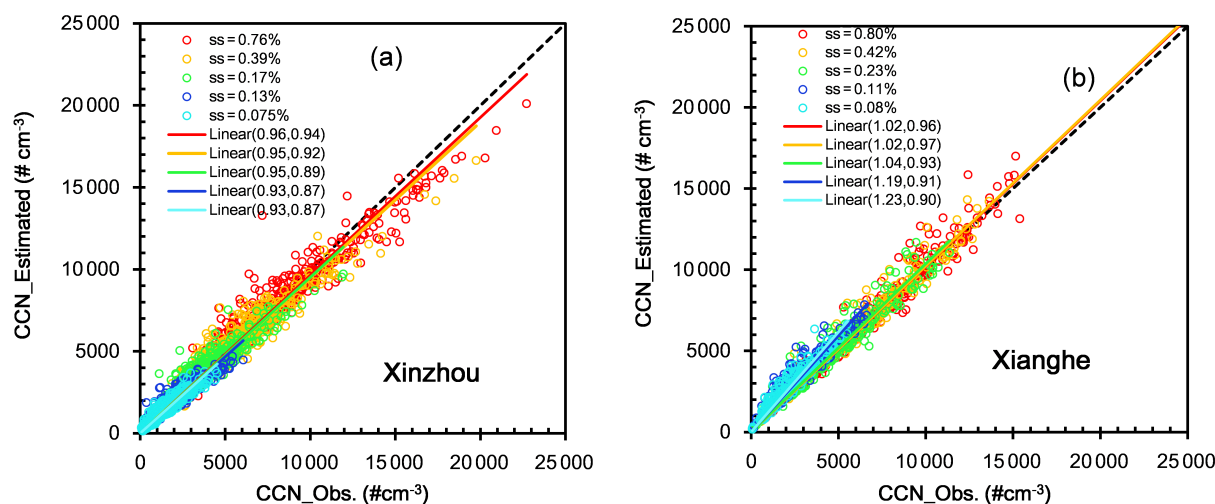


Figure 7. Estimated N_{CCN} as a function of observed N_{CCN} for different supersaturation levels at (a) Xinzhou and (b) Xianghe. Note that the campaign mean CCN efficiency spectra at Xinzhou are used for estimating N_{CCN} at Xianghe. Linear best-fit lines through each group of points are shown. Slopes and R^2 values are given in parentheses.

was underestimated by 11 and 4 %, respectively, at $f_{44} < 11$ and $f_{44} > 15$ %. The results showed that the estimation of N_{CCN} would be largely improved if the aerosol particles were aged with high oxidation level, especially when the chemical composition of the particles is dominated by organics. However, for the particles with relative low organics ($x_{org} < 40$ %), the effect caused by the f_{44} was quite insignificant both for high and low supersaturations. In Fig. 6, the slopes were all around 1.0 at the two cases of $f_{44} < 11$ and $f_{44} > 15$ %. This can be easily explained. When x_{org} is less than 40 %, the overall hygroscopicity of the particles is dominated by inorganic species such as sulfate and nitrate, which are more hygroscopic (κ_{inorg} usually larger than 0.6) than organic compounds (κ_{org} usually smaller than 0.2). As a result, a larger fraction of particles can be activated. According to the simple mixing rule based on chemical volume fractions proposed by Petters and Kreidenweis (2007), the contribution from organics is quite small. If x_{org} is greater than 60 %, organics will dominate the overall particle hygroscopicity. Particles with a large f_{44} are much more hygroscopic and thus more CCN-active. Our results indicated that increasing the proportion of secondary organics would decrease the uncertainties in estimating N_{CCN} and lead to a more accurate estimation of N_{CCN} .

4.5 Applicability of CCN efficiency spectra

As a means of testing the applicability of the CCN activation spectra, campaign mean CCN efficiency spectra at different supersaturations observed at the Xinzhou site are used to estimate N_{CCN} at the Xinzhou and Xianghe sites, respectively, which helps to further examine the sensitivity of N_{CCN} to aerosol type. Data from the two sites were measured during the warm season so that the effect of temporal varia-

tions in aerosols on CCN levels is reduced. Fitted campaign mean CCN efficiency spectra at the five supersaturations at Xinzhou (corresponding to spectra in Fig. 1) are multiplied by dry PSDs actually measured at the Xinzhou and Xianghe sites, respectively. This generates estimated CCN size distributions at the two sites. They are then integrated over the whole size range (14–600 and 10–700 nm at the Xinzhou and Xianghe sites, respectively) to obtain the estimated N_{CCN} . The measured CCN size distributions at each site are integrated to produce the observed N_{CCN} .

Figure 7 shows estimated N_{CCN} as a function of measured N_{CCN} for different supersaturation levels at the two sites. N_{CCN} at Xinzhou was underestimated by 4–5 % at supersaturation levels of 0.39 and 0.76 % and was slightly overestimated (~ 2 %) at Xianghe for the same supersaturation levels. Good agreement is seen at the 0.39 and 0.76 % supersaturation levels for data from both sites ($R^2 > 0.92$). N_{CCN} at Xinzhou was underestimated by ~ 7 % at supersaturation levels < 0.1 % ($R^2 = 0.87$). At Xianghe, however, N_{CCN} was overestimated by 19–23 % at supersaturation levels < 0.1 % although the correlation between calculated and measured N_{CCN} was good. Because size-resolved CCN efficiency spectra were applied here, excluding the impact of particle size, the influence of chemical composition on CCN activation can be investigated. The poor estimates of CCN at low supersaturation levels could be attributed to the high sensitivity of N_{CCN} to chemical composition. Because the mass fractions of inorganics and organics measured at the two sites are similar (Fig. 1) and the hygroscopicity for inorganic components is fixed, this overestimation is attributed to the smaller proportion of aged and oxidized organic aerosols at Xianghe compared with aerosols at Xinzhou ($f_{44} = 17$ and 11 % at Xinzhou and Xianghe, respectively).

5 Summary and conclusions

In this study, we have investigated the impacts of particle physicochemical properties on CCN activity based on field measurements obtained from 22 July to 26 August of 2014 in the suburb of Xinzhou, China. Five-day back trajectories combined with measurements were analyzed to examine air mass influences on CCN activity. CCN efficiency was largely reduced by local air masses, and the MAF was low to < 60 %, suggesting externally mixed and heterogeneous particle composition for local emitted aerosols. The CCN activation efficiency was enhanced significantly when the site was under the influence of air transported from far away, during which aerosols could be mixed well with more hygroscopic secondary organic and inorganic components. The relationship between N_{CN} and N_{CCN} was generally poor. Large errors would arise if using the former to estimate the latter, especially under low supersaturation conditions.

The sensitivity of N_{CCN} estimation to both x_{org} and f_{44} has also been examined. A strong dependence of N_{CCN} on the both two parameters was noted. The sensitivity of N_{CCN} to volume fraction and particles oxidation or aging level of organics increased with increase of x_{org} . This dependence also weakens as the supersaturation level increases. When the particles were mostly composed of organics ($x_{\text{org}} > 60\%$), the N_{CCN} at the supersaturation of 0.075 and 0.13 % was underestimated by 46 and 44 %, respectively, if aerosol particles were freshly emitted with primary organics ($f_{44} < 11\%$), while the underestimation decreased to 32 and 23 % at the corresponding supersaturations if the particles were with more hygroscopic secondary organics ($f_{44} > 15\%$). The N_{CCN} at the supersaturation of 0.76 % was underestimated by 11 and 4 %, respectively, at $f_{44} < 11$ and $f_{44} > 15\%$. However, for the particles composed of low organics (e.g., $x_{\text{org}} < 40\%$), the effect caused by the f_{44} was quite insignificant both at high and low supersaturations. This is due to that the overall hygroscopicity of the particles is dominated by inorganics such as sulfate and nitrate, which are more hygroscopic than organic compounds. Our results indicated that it would lead to a more accurate estimation of N_{CCN} to increase the proportion of secondary organics, especially when the composition of the aerosols is dominated by organics.

The applicability of the CCN efficiency spectrum measured at the Xinzhou site to the Xianghe site was examined and a good agreement was found when the supersaturation level was > 0.2 %. However, N_{CCN} at the Xianghe site was overestimated by 19–23 % when the supersaturation level was < 0.1 %. Because of the similar mass fractions of inorganics and organics measured at the two sites, we conclude that this overestimation was mainly caused by the smaller proportion of aged and oxidized organic aerosols at Xianghe compared to aerosols at Xinzhou.

Acknowledgements. This work was funded by the National Basic Research Program of China “973” (grant nos. 2013CB955801, 2013CB955804), the NSF (China) (grant nos. 4141101031, 91544217), and NSF (USA) (AGS1118325 and 1534670). We also acknowledge the members of the A²C² team for their hard work during the campaign, including Du Wei (from the State Key Laboratory of Atmospheric Boundary Layer Physics and Atmospheric Chemistry of the Institute of Atmospheric Physics/Chinese Academy of Sciences for carrying out the chemical composition measurements) and Yuan Cheng (from Nanjing University who helped make the size-resolved CCNc measurements).

Edited by: X. Liu

References

- Aiken, A. C., DeCarlo, P. F., Kroll, J. H., Worsnop, D. R., Huffman, J. A., Docherty, K. S., Ulbrich, I. M., Mohr, C., Kimmel, J. R., Sueper, D., Sun, Y., Zhang, Q., Tramborn, A., Northway, M., Ziemann, P. J., Canagaratna, M. R., Onasch, T. B., Alfarra, M. R., Prevot, A. S. H., Dommen, J., Duplissy, J., Metzger, A., Baltensperger, U., and Jimenez, J. L.: O/C and OM/OC ratios of primary, secondary, and ambient organic aerosols with high-resolution time-of-flight aerosol mass spectrometry, *Environ. Sci. Technol.*, 42, 4478–4485, 2008.
- Andreae, M. O.: Correlation between cloud condensation nuclei concentration and aerosol optical thickness in remote and polluted regions, *Atmos. Chem. Phys.*, 9, 543–556, doi:10.5194/acp-9-543-2009, 2009.
- Bougiatioti, A., Fountoukis, C., Kalivitis, N., Pandis, S. N., Nenes, A., and Mihalopoulos, N.: Cloud condensation nuclei measurements in the marine boundary layer of the Eastern Mediterranean: CCN closure and droplet growth kinetics, *Atmos. Chem. Phys.*, 9, 7053–7066, doi:10.5194/acp-9-7053-2009, 2009.
- Bougiatioti, A., Nenes, A., Fountoukis, C., Kalivitis, N., Pandis, S. N., and Mihalopoulos, N.: Size-resolved CCN distributions and activation kinetics of aged continental and marine aerosol, *Atmos. Chem. Phys.*, 11, 8791–8808, doi:10.5194/acp-11-8791-2011, 2011.
- Chuang, P. Y., Collins, D. R., Pawlowska, H., Snider, J. R., Jonsson, H. H., Brenguier, J. L., Flagan, R. C., and Seinfeld, J. H.: CCN measurements during ACE-2 and their relationship to cloud microphysical properties, *Tellus B*, 52, 843–867, 2000.
- Clarke, A., McNaughton, C., Kasputin, V. N., Shinozuka, Y., Howell, S., Dibb, J., Zhou, J., Anderson, B., Brekhovskikh, V., Turner, H., and Pinkerton, M.: Biomass burning and pollution aerosol over North America: Organic components and their influence on spectral optical properties and humidification response, *J. Geophys. Res.*, 112, D12S18, doi:10.1029/2006JD007777, 2007.
- Dal Maso, M., Sogacheva, L., Aalto, P. P., Riipinen, I., Komppula, M., Tunved, P., Korhonen, L., Suuruskki, V., Hirsikko, A., and Kurten, T.: Aerosol size distribution measurements at four Nordic field stations: identification, analysis and trajectory analysis of new particle formation bursts, *Tellus B*, 59, 350–361, 2007.
- Deng, Z. Z., Zhao, C. S., Ma, N., Liu, P. F., Ran, L., Xu, W. Y., Chen, J., Liang, Z., Liang, S., Huang, M. Y., Ma, X. C., Zhang, Q., Quan, J. N., Yan, P., Henning, S., Mildenberger, K., Sommerhage, E., Schäfer, M., Stratmann, F., and Wiedensohler,

- A.: Size-resolved and bulk activation properties of aerosols in the North China Plain, *Atmos. Chem. Phys.*, 11, 3835–3846, doi:10.5194/acp-11-3835-2011, 2011.
- Deng, Z. Z., Zhao, C. S., Ma, N., Ran, L., Zhou, G. Q., Lu, D. R., and Zhou, X. J.: An examination of parameterizations for the CCN number concentration based on in situ measurements of aerosol activation properties in the North China Plain, *Atmos. Chem. Phys.*, 13, 6227–6237, doi:10.5194/acp-13-6227-2013, 2013.
- Draxler, R. R. and Hess, G. D.: An overview of the HYSPLIT 4 modeling system for trajectories, dispersion, and deposition, *Aust. Meteorol. Mag.*, 47, 295–308, 1998.
- Duplissy, J., DeCarlo, P. F., Dommen, J., Alfarra, M. R., Metzger, A., Barmapadimos, I., Prevot, A. S. H., Weingartner, E., Tritscher, T., Gysel, M., Aiken, A. C., Jimenez, J. L., Canagaratna, M. R., Worsnop, D. R., Collins, D. R., Tomlinson, J., and Baltensperger, U.: Relating hygroscopicity and composition of organic aerosol particulate matter, *Atmos. Chem. Phys.*, 11, 1155–1165, doi:10.5194/acp-11-1155-2011, 2011.
- Dusek, U., Covert, D. S., Wiedensohler, A., Neususs, C., Weise, D., and Cantrell, W.: Cloud condensation nuclei spectra derived from size distributions and hygroscopic properties of the aerosol in coastal south-west Portugal during ACE-2, *Tellus B*, 55, 35–53, 2003.
- Engelhart, G. J., Hennigan, C. J., Miracolo, M. A., Robinson, A. L., and Pandis, S. N.: Cloud condensation nuclei activity of fresh primary and aged biomass burning aerosol, *Atmos. Chem. Phys.*, 12, 7285–7293, doi:10.5194/acp-12-7285-2012, 2012.
- Ervens, B., Cubison, M. J., Andrews, E., Feingold, G., Ogren, J. A., Jimenez, J. L., Quinn, P. K., Bates, T. S., Wang, J., Zhang, Q., Coe, H., Flynn, M., and Allan, J. D.: CCN predictions using simplified assumptions of organic aerosol composition and mixing state: a synthesis from six different locations, *Atmos. Chem. Phys.*, 10, 4795–4807, doi:10.5194/acp-10-4795-2010, 2010.
- Gasparini, R., Collins, D. R., Andrews, E., Sheridan, P. J., Ogren, J. A., and Hudson, J. G.: Coupling aerosol size distributions and size-resolved hygroscopicity to predict humidity-dependent optical properties and cloud condensation nuclei spectra, *J. Geophys. Res.*, 111, D05S13, doi:10.1029/2005JD006092, 2006.
- Gunthe, S. S., Rose, D., Su, H., Garland, R. M., Achtert, P., Nowak, A., Wiedensohler, A., Kuwata, M., Takegawa, N., Kondo, Y., Hu, M., Shao, M., Zhu, T., Andreae, M. O., and Pöschl, U.: Cloud condensation nuclei (CCN) from fresh and aged air pollution in the megacity region of Beijing, *Atmos. Chem. Phys.*, 11, 11023–11039, doi:10.5194/acp-11-11023-2011, 2011.
- Guo, S., Hu, M., Zamora, M. L., Peng, J., Shang, D., Zheng, J., Zhuofei, D., Zhijun, W., Min, S., Zeng, L., Molina, M. J., and Zhang, R.: Elucidating severe urban haze formation in China, *P. Natl. Acad. Sci. USA*, 111, 17373–17378, doi:10.1073/pnas.1419604111, 2014.
- Hartz, K. E. H., Tischuk, J. E., Chan, M. N., Chan, C. K., Donahue, N. M., and Pandis, S. N.: Cloud condensation nuclei activation of limited solubility organic aerosol, *Atmos. Environ.*, 40, 605–617, 2006.
- Hings, S. S., Wrobel, W. C., Cross, E. S., Worsnop, D. R., Davidovits, P., and Onasch, T. B.: CCN activation experiments with adipic acid: effect of particle phase and adipic acid coatings on soluble and insoluble particles, *Atmos. Chem. Phys.*, 8, 3735–3748, doi:10.5194/acp-8-3735-2008, 2008.
- Hudson, J. G. and Da, X. Y.: Volatility and size of cloud condensation nuclei, *J. Geophys. Res.*, 101, 4435–4442, 1996.
- Hussein, T., Dal Maso, M., Petäjä, T., Koponen, I. K., Paatero, P., Aalt, P. P., Hämeri, K., and Kulmala, M.: Evaluation of an automatic algorithm for fitting the particle number size distributions, *Boreal Environ. Res.*, 10, 337–355, 2005.
- Kammermann, L., Gysel, M., Weingartner, E., Herich, H., Cziczo, D. J., Holst, T., Svenningsson, B., Arneth, A., and Baltensperger, U.: Subarctic atmospheric aerosol composition: 3. Measured and modeled properties of cloud condensation nuclei, *J. Geophys. Res.*, 115, D04202, doi:10.1029/2009JD012447, 2010.
- Köhler, H.: The nucleus in and growth of hygroscopic droplets, *Trans. Faraday Soc.*, 32, 1152–1161, doi:10.1039/TF9363201152, 1936.
- Lance, S., Medina, J., Smith, J., and Nenes, A.: Mapping the operation of the DMT continuous flow CCN counter, *Aerosol Sci. Technol.*, 40, 242–254, 2006.
- Latham, T. L., Beyersdorf, A. J., Thornhill, K. L., Winstead, E. L., Cubison, M. J., Hecobian, A., Jimenez, J. L., Weber, R. J., Anderson, B. E., and Nenes, A.: Analysis of CCN activity of Arctic aerosol and Canadian biomass burning during summer 2008, *Atmos. Chem. Phys.*, 13, 2735–2756, doi:10.5194/acp-13-2735-2013, 2013.
- Lee, Y. S., Collins, D. R., Li, R. J., Bowman, K. P., and Feingold, G.: Expected impact of an aged biomass burning aerosol on cloud condensation nuclei and cloud droplet concentrations, *J. Geophys. Res.*, 111, D22204, doi:10.1029/2005JD006464, 2006.
- Li, Z., Chen, H., Cribb, M., Dickerson, R. E., Holben, B., Li, C., Lu, D., Luo, Y., Maring, H., Shi, G., Tsay, S.-C., Wang, P., Wang, Y., Xia, X., Zheng, Y., Yuan, T., and Zhao, F.: Preface to special section on East Asian Studies of Tropospheric Aerosols: An International Regional Experiment (EASTAIRE), *J. Geophys. Res.*, 112, D22S00, doi:10.1029/2007JD008853, 2007.
- Li, Z., Li, C., Chen, H., Tsay, S.-C., Holben, B., Huang, J., Li, B., Maring, H., Qian, Y., Shi, G., Xia, X., Yin, Y., Zheng, Y., and Zhuang, G.: East Asian Studies of Tropospheric Aerosols and Impact on Regional Climate (EAST©): An overview, *J. Geophys. Res.*, 116, D00K34, doi:10.1029/2010JD015257, 2011.
- Liu, X. and Wang, J.: How important is organic aerosol hygroscopicity to aerosol indirect forcing? *Environ. Res. Lett.*, 5, 44010–44019, doi:10.1088/1748-9326/5/4/044010, 2010.
- McFiggans, G., Artaxo, P., Baltensperger, U., Coe, H., Facchini, M. C., Feingold, G., Fuzzi, S., Gysel, M., Laaksonen, A., Lohmann, U., Mentel, T. F., Murphy, D. M., O’Dowd, C. D., Snider, J. R., and Weingartner, E.: The effect of physical and chemical aerosol properties on warm cloud droplet activation, *Atmos. Chem. Phys.*, 6, 2593–2649, doi:10.5194/acp-6-2593-2006, 2006.
- Mei, F., Setyan, A., Zhang, Q., and Wang, J.: CCN activity of organic aerosols observed downwind of urban emissions during CARES, *Atmos. Chem. Phys.*, 13, 12155–12169, doi:10.5194/acp-13-12155-2013, 2013a.
- Mei, F., Hayes, P. L., Ortega, A. M., Taylor, J. W., Allan, J. D., Gilman, J. B., Kuster, W. C., de Gouw, J. A., Jimenez, J. L., and Wang, J.: Droplet activation properties of organic aerosols observed at an urban site during CalNex-LA, *J. Geophys. Res.*, 118, 2903–2917, doi:10.1002/jgrd.50285, 2013b.
- Mircea, M., Facchini, M. C., Decesari, S., Cavalli, F., Emblico, L., Fuzzi, S., Vestin, A., Rissler, J., Swietlicki, E., Frank, G., Andreae, M. O., Maenhaut, W., Rudich, Y., and Artaxo, P.: Impor-

- tance of the organic aerosol fraction for modeling aerosol hygroscopic growth and activation: a case study in the Amazon Basin, *Atmos. Chem. Phys.*, 5, 3111–3126, doi:10.5194/acp-5-3111-2005, 2005.
- Ng, N. L., Herndon, S. C., Trimborn, A., Canagaratna, M. R., Croteau, P. L., Onasch, T. B., Sueper, D., Worsnop, D. R., Zhang, Q., Sun, Y. L., and Jayne, J. T.: An Aerosol Chemical Speciation Monitor (ACSM) for Routine Monitoring of the Composition and Mass Concentrations of Ambient Aerosol, *Aerosol Sci. Technol.*, 45, 770–784, 2011.
- Paramonov, M., Aalto, P. P., Asmi, A., Prisle, N., Kerminen, V.-M., Kulmala, M., and Petäjä, T.: The analysis of size-segregated cloud condensation nuclei counter (CCNC) data and its implications for cloud droplet activation, *Atmos. Chem. Phys.*, 13, 10285–10301, doi:10.5194/acp-13-10285-2013, 2013.
- Petters, M. D. and Kreidenweis, S. M.: A single parameter representation of hygroscopic growth and cloud condensation nucleus activity, *Atmos. Chem. Phys.*, 7, 1961–1971, doi:10.5194/acp-7-1961-2007, 2007.
- Raymond, T. M. and Pandis, S. N.: Cloud activation of single component organic aerosol particles, *J. Geophys. Res.*, 107, 4787, doi:10.1029/2002JD002159, 2002.
- Reutter, P., Su, H., Trentmann, J., Simmel, M., Rose, D., Gunthe, S. S., Wernli, H., Andreae, M. O., and Pöschl, U.: Aerosol- and updraft-limited regimes of cloud droplet formation: influence of particle number, size and hygroscopicity on the activation of cloud condensation nuclei (CCN), *Atmos. Chem. Phys.*, 9, 7067–7080, doi:10.5194/acp-9-7067-2009, 2009.
- Rissler, J., Swietlicki, E., Zhou, J., Roberts, G., Andreae, M. O., Gatti, L. V., and Artaxo, P.: Physical properties of the sub-micrometer aerosol over the Amazon rain forest during the wet-to-dry season transition – comparison of modeled and measured CCN concentrations, *Atmos. Chem. Phys.*, 4, 2119–2143, doi:10.5194/acp-4-2119-2004, 2004.
- Rissler, J., Vestin, A., Swietlicki, E., Fisch, G., Zhou, J., Artaxo, P., and Andreae, M. O.: Size distribution and hygroscopic properties of aerosol particles from dry-season biomass burning in Amazonia, *Atmos. Chem. Phys.*, 6, 471–491, doi:10.5194/acp-6-471-2006, 2006.
- Rose, D., Gunthe, S. S., Mikhailov, E., Frank, G. P., Dusek, U., Andreae, M. O., and Pöschl, U.: Calibration and measurement uncertainties of a continuous-flow cloud condensation nuclei counter (DMT-CCNC): CCN activation of ammonium sulfate and sodium chloride aerosol particles in theory and experiment, *Atmos. Chem. Phys.*, 8, 1153–1179, doi:10.5194/acp-8-1153-2008, 2008.
- Rose, D., Nowak, A., Achtert, P., Wiedensohler, A., Hu, M., Shao, M., Zhang, Y., Andreae, M. O., and Pöschl, U.: Cloud condensation nuclei in polluted air and biomass burning smoke near the mega-city Guangzhou, China – Part 1: Size-resolved measurements and implications for the modeling of aerosol particle hygroscopicity and CCN activity, *Atmos. Chem. Phys.*, 10, 3365–3383, doi:10.5194/acp-10-3365-2010, 2010.
- Rousseau, D. D., Duzer, D., Etienne, J. L., Cambon, G., Jolly, D., Ferrier, J., and Schevin, P.: Pollen record of rapidly changing air trajectories to the North Pole, *J. Geophys. Res.*, 109, D06116, doi:10.1029/2003JD003985, 2004.
- Snider, J. R., Guibert, S., Brenguierand, J. L., and Putaud, J. P.: Aerosol activation in marine stratocumulus clouds: Part II – Köhler and parcel theory closure studies, *J. Geophys. Res.*, 108, 8629, doi:10.1029/2002JD002692, 2003.
- Sotiropoulou, R. E. P., Nenes, A., Adams, P. J., and Seinfeld, J. H.: Cloud condensation nuclei prediction error from application of Köhler theory: Importance for the aerosol indirect effect, *J. Geophys. Res.*, 112, D12202, doi:10.1029/2006JD007834, 2007.
- Stohl, A.: Trajectory statistics – a new method to establish source-receptor relationships of air pollutants and its application to the transport of particulate sulfate in Europe, *Atmos. Environ.*, 30, 579–587, 1996.
- Stroud, C. A., Nenes, A., Jimenez, J. L., DeCarlo, P., Huffman, J. A., Bruinjtes, R., Nemitz, E., Delia, A. E., Toohey, D. W., Guenther, A. B., and Nandi, S.: Cloud Activating Properties of Aerosol Observed during CELTIC, *J. Atmos. Sci.*, 64, 441–459, 2007.
- Sun, Y., Wang, Z., Dong, H., Yang, T., Li, J., Pan, X., Chen, P., and Jayne, J. T.: Characterization of summer organic and inorganic aerosols in Beijing, China with an Aerosol Chemical Speciation Monitor, *Atmos. Environ.*, 51, 250–259, doi:10.1016/j.atmosenv.2012.01.013, 2012.
- Takegawa, N., Miyakawa, T., Kawamura, K., and Kondo, Y.: Contribution of selected di-carboxylic and omega-oxocarboxylic acids in ambient aerosol to the m/z 44 signal of an aerodyne aerosol mass spectrometer, *Aerosol Sci. Technol.*, 41, 418–437, doi:10.1080/02786820701203215, 2007.
- Twohy, C. H. and Anderson, J. R.: Droplet nuclei in non-precipitating clouds: composition and size matter, *Environ. Res. Lett.*, 3, 045002, doi:10.1088/1748-9326/3/4/045002, 2008.
- VanReken, T. M., Rissman, T. A., Roberts, G. C., Varutbangkul, V., Jonsson, H. H., Flagan, R. C., and Seinfeld, J. H.: Toward aerosol/cloud condensation nuclei (CCN) closure during CRYSTAL-FACE, *J. Geophys. Res.*, 108, 1769–1778, doi:10.1029/2003JD003582, 2003.
- VanReken, T. M., Ng, N. L., Flagan, R. C., and Seinfeld, J. H.: Cloud condensation nucleus activation properties of biogenic secondary organic aerosol, *J. Geophys. Res.*, 110, D07206, doi:10.1029/2004JD005465, 2005.
- Varutbangkul, V., Brechtel, F. J., Bahreini, R., Ng, N. L., Keywood, M. D., Kroll, J. H., Flagan, R. C., Seinfeld, J. H., Lee, A., and Goldstein, A. H.: Hygroscopicity of secondary organic aerosols formed by oxidation of cycloalkenes, monoterpenes, sesquiterpenes, and related compounds, *Atmos. Chem. Phys.*, 6, 2367–2388, doi:10.5194/acp-6-2367-2006, 2006.
- Verver, G., Raes, F., Voegelzang, D., and Johnson, D.: The 2nd Aerosol characterization Experiment (ACE-2): meteorological and chemical context, *Tellus B*, 52, 126–140, 2000.
- Wang, J., Lee, Y.-N., Daum, P. H., Jayne, J., and Alexander, M. L.: Effects of aerosol organics on cloud condensation nucleus (CCN) concentration and first indirect aerosol effect, *Atmos. Chem. Phys.*, 8, 6325–6339, doi:10.5194/acp-8-6325-2008, 2008.
- Wang, Y. Q., Zhang, X. Y., and Draxler, R.: TrajStat: GIS-based software that uses various trajectory statistical analysis methods to identify potential sources from long-term air pollution measurement data, *Environ. Modell. Softw.*, 24, 938–939, 2009.
- Ward, D. S., Eidhammer, T., Cotton, W. R., and Kreidenweis, S. M.: The role of the particle size distribution in assessing aerosol composition effects on simulated droplet activation, *Atmos. Chem. Phys.*, 10, 5435–5447, doi:10.5194/acp-10-5435-2010, 2010.
- Weber, R., McMurry, P. H., Mauldin, R., Tanner, D., Eisele, F., Clarke, A., and Kapustin, V.: New particle formation in the re-

- mote troposphere: A comparison of observations at various sites, *Geophys. Res. Lett.*, 26, 307–310, 1999.
- Wex, H., Hennig, T., Salma, I., Ocskay, R., Kiselev, A., Henning, S., Massling, A., Wiedensohler, A., and Stratmann, F.: Hygroscopic growth and measured and modeled critical super-saturations of an atmospheric HULIS sample, *Geophys. Res. Lett.*, 34, L02818, doi:10.1029/2006GL028260, 2007.
- Whitby, K., T.: The physical characteristics of sulfur aerosols, *Atmos. Environ.*, 12, 135–159, 1967, 1978.
- Wiedensohler, A., Cheng, Y. F., Nowak, A., Wehner, B., Achtert, P., Berghof, M., Birmili, W., Wu, Z. J., Hu, M., Zhu, T., Takegawa, N., Kita, K., Kondo, Y., Lou, S. R., Hofeumahaus, A., Holland, F., Wahner, A., Gunthe, S. S., Rose, D., Su, H., and Pöschl, U.: Rapid aerosol particle growth and increase of cloud condensation nucleus activity by secondary aerosol formation and condensation: A case study for regional air pollution in northeastern China, *J. Geophys. Res.-Atmos.*, 114, 1283–1289, doi:10.1029/2008JD010884, 2009.
- Yue, D. L., Hu, M., Zhang, R. J., Wu, Z. J., Su, H., Wang, Z. B., Peng, J. F., He, L. Y., Huang, X. F., Gong, Y. G., and Wiedensohler, A.: Potential contribution of new particle formation to cloud condensation nuclei in Beijing, *Atmos. Environ.*, 45, 6070–6077, 2011.
- Zhang, Q., Meng, J., Quan, J., Gao, Y., Zhao, D., Chen, P., and He, H.: Impact of aerosol composition on cloud condensation nuclei activity, *Atmos. Chem. Phys.*, 12, 3783–3790, doi:10.5194/acp-12-3783-2012, 2012.
- Zhang, F., Li, Y., Li, Z., Sun, L., Li, R., Zhao, C., Wang, P., Sun, Y., Liu, X., Li, J., Li, P., Ren, G., and Fan, T.: Aerosol hygroscopicity and cloud condensation nuclei activity during the AC3Exp campaign: implications for cloud condensation nuclei parameterization, *Atmos. Chem. Phys.*, 14, 13423–13437, doi:10.5194/acp-14-13423-2014, 2014.